

## SOME SIMILARITIES AND DIFFERENCES BETWEEN THE MARS AND VENUS SOLAR WIND INTERACTIONS

JEAN-GABRIEL TROTIGNON

*Laboratoire de Physique et Chimie de l'Environnement, Centre National de la  
Recherche Scientifique, Orléans University  
3A, Avenue de la Recherche Scientifique, F-45071 Orléans Cedex 02, France  
jean-gabriel.trotignon@cnr-s-orleans.fr*

The plasma environments of Mars and Venus have been explored by spacecraft, such as Mars 2, 3 and 5, Phobos 2, Mars Global Surveyor (MGS), Mars Express for planet Mars and Venera 9 and 10, Pioneer Venus Orbiter, Venus Express for planet Venus. Overall observations of plasma regions and their boundaries, in particular the bow shock, the magnetic pile-up boundary and the magnetic tail, show the solar wind interaction with these two planets to be rather similar. Mars and Venus are both considered as non-magnetic planets, compared with the Earth, in a sense that they do not possess any significant intrinsic magnetic field that could play a significant role in their interactions with the solar wind. At most, the magnetic anomalies discovered at Mars by MGS are thought to slightly influence the lower regions of the Martian ionosphere. Therefore, both Venus and Mars have principally comet-like induced magnetospheres and magnetotails as a result of the atmospheric mass loading and subsequent draping of passing interplanetary flux tubes. Nevertheless, there are many differences between the characteristics and space environment behaviors of the two telluric planets and a lot remains actually to be done, in terms of *in situ* measurements and modeling efforts, to fully understand how Venus and Mars interact with the interplanetary medium. The objective of the presentation is not to review all the aspects of these interactions but simply to compare the main characteristics of the Mars' and Venus' plasma environments and to highlight some similarities and differences between the interactions of these two non-magnetic planets with the solar wind as a function of solar wind dynamic pressure and solar activity.

### 1. Introduction

Despite the great number of missions devoted to the exploration of Earth's nearest neighbors, Venus and Mars and a prolific scientific output, actually not too much is known about the interaction of these planets with the solar

wind, and this is particularly true for Mars. This is due to limitations of space missions for gathering *in situ* data especially in situation involving variations in latitude, longitude, altitude, time, and solar activity. This is also because only a very few spacecraft are well equipped to monitor electric and magnetic fields, and the spatial distribution and composition of particles over wide ranges of frequency, mass and energy. This leads one to the conclusion that new missions, in particular low altitude orbiters and entry probes, are required to fully understand the nature of these interactions, compared with the ones of the Earth and mainly comets. They are indeed thought to be much more intricate than those described in most of the current literature.

The objective of this paper is actually not to give a comprehensive review of what is known and what is unknown about the plasma and wave environments of Mars and Venus and about their interactions with the interplanetary medium but rather to point out some relevant features that remains to be clarified and/or understood and therefore investigated in future missions.

Section 2 recalls the basic facts about the interactions between the solar wind and the two planets. Some major similarities and differences are then presented in Sec. 3, before the conclusion.

## 2. Basic Facts about Venus and Mars Solar Wind Interactions

### 2.1. *The Venus case*

Venera 9 and 10 and Pioneer Venus Orbiter (PVO) missions to Venus have considerably enriched our knowledge of the space environment of Venus and its interaction with the solar wind.<sup>1,2</sup>

Venus turned out to be a non-magnetic planet, with a dense dayside ionosphere. There are extended dayside exospheres of hot hydrogen and oxygen: O dominates over H up to 3000 km where H becomes dominant (the main source of neutral O corona is dissociative recombination of  $O_2^+$ ). Neutral exosphere atoms above the dayside ionopause, ionized by photoionization, charge exchange with solar wind protons, impact ionization, etc., can mass load and slow the solar wind via pickup processes, as for comets.

Venus has no intrinsic magnetic field that could stand off the solar wind. The solar wind thus appears to be diverted around the upper boundary of the ionosphere, the ionopause, where the incident solar wind ram pressure is balanced by the ionosphere thermal pressure. At the

ionopause, dissipationless currents flow in a thin layer, thus creating a highly conducting spheroid. These currents produce magnetic fields that contribute to stand off the solar wind.

As illustrated in Fig. 1,<sup>1</sup> the solar wind is shocked and diverted around the ionosphere and continues along its antisolar route. This flow carries the interplanetary magnetic field with it. The interplanetary magnetic field is compressed in front of the Venus' ionopause, thus creating a magnetic barrier that separates the plasmas of external and internal origin. On the flanks of the planet, the interplanetary magnetic field lines continue to move downward to form a magnetic tail similar to comet tails. This phenomenon is known as the magnetic field draping effect.

## 2.2. The Mars case

Before Mars Global Surveyor (MGS), the only available measurements of the upper environment of Mars come from spacecraft *en route* to deliver landers and higher-altitude data from orbiters which never encountered the ionosphere.<sup>3</sup> This explains why a controversy has long existed regarding the nature of the Martian obstacle to the solar wind flow. The MGS data have confirmed that it is an ionospheric obstacle like that of the unmagnetized

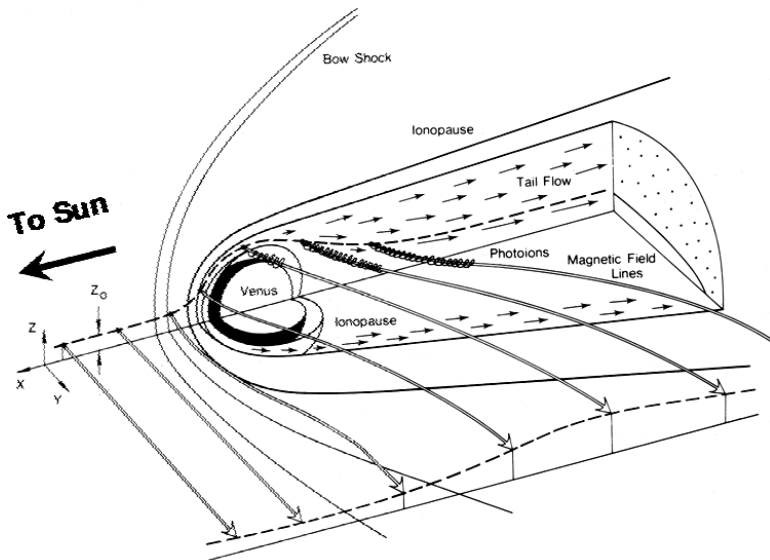


Fig. 1. Formation of induced Venus' magnetotail from draped interplanetary magnetic field.<sup>1</sup>

planet Venus, while multiple magnetic anomalies of small spatial scale exist in the crust of Mars.<sup>4</sup> These magnetic anomalies are at most thought to slightly influence the lower regions of the Martian ionosphere.<sup>5</sup> The low Martian gravitational field (compared with those of Earth and Venus) allows the neutral exosphere of Mars to interact significantly with the interplanetary medium. Comet-like features are likely to be more evident at Mars than Venus.<sup>6</sup>

Neutral particles can escape above the exobase ( $\sim 200$ -km altitude): those whose velocities are larger than  $5 \text{ km s}^{-1}$ , the required velocity for escape from Mars, will contribute to the solar wind erosion of the Mars atmosphere; the others make up the gravitationally bound exosphere. Particles can gain energy through photochemical processes or sputtering by energetic particles from above. For example,  $\text{O}_2^+$  which are majority ions in the ionosphere of Mars produce energetic oxygen atoms,  $\text{O}^*$ , through photodissociative recombination.  $\text{O}^*$  may gain sufficient energy to flow sunward and even escape from Mars. At Venus, the above photodissociative recombination cannot supply  $\text{O}^*$  whose velocity is larger than the Venus escape velocity ( $\sim 10 \text{ km s}^{-1}$ ). By photoionization  $\text{O}^+$  ions may then be produced and captured by the solar wind and embedded into the interplanetary magnetic field (ion pickup process as for Venus and comets). As ions are continuously produced, the solar wind carries more material along with it and is mass-loaded. Conservation of momentum and energy implies a slowing down of the solar wind flow, thus diminishing the pressure exerted on the planet environment. Extensive reviews of the Martian environment and its interaction with the solar wind may be found in Refs. 3 and 7–9 and references therein.

### 3. Some Similarities and Differences

#### 3.1. *Bow shock and upstream waves*

Figure 2 shows the Venus' and Mars' bow shock models inferred from the data of, respectively, PVO,<sup>10</sup> and Phobos 2 and MGS.<sup>11</sup>

As can be seen in Fig. 2, the Mars' bow shock has a larger terminator radius than the one of Venus, while the subsolar positions of the two bow shocks are comparable. In addition, the effective obstacle to the solar wind flow is larger at the flanks of Mars. According to Luhmann,<sup>12</sup> it could be the result of a larger solar wind ion gyroradius relative to the planet radius for Mars and/or different compositions and scale heights of the two upper atmospheres.

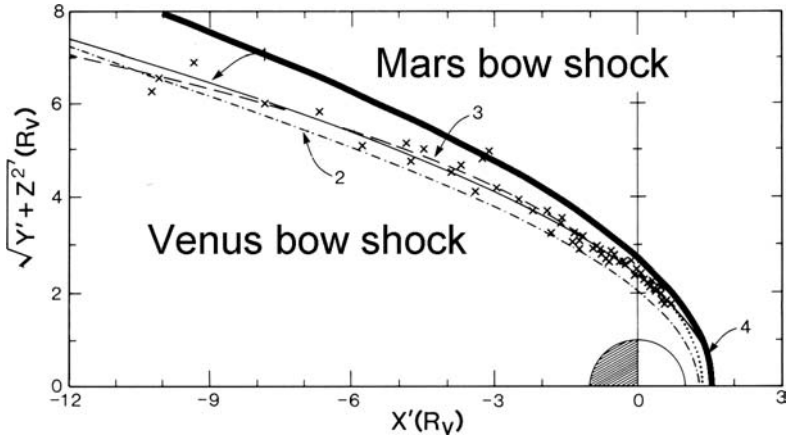


Fig. 2. Conic section fits to the positions of the Venus bow shock crossed by PVO (thin solid, dashed and dashed-dotted lines).<sup>10</sup> For comparison, the conic section fit to the Mars bow shock positions obtained from the Phobos 2 and MGS observations is shown as a thick solid line.<sup>11</sup> For the latter curve,  $R_V$  must be replaced by  $R_M$ , the Martian radius.

The electric-field spectra plotted in the right-hand panel of Fig. 3 were recorded in the Martian bow shock ramp by the Plasma Wave System (PWS) onboard Phobos 2. These spectra exhibit two main components: a low-frequency component, below the electron cyclotron frequency,  $f_{ce}$ , which is attributed to the electric component of the whistler mode noise; and a high-frequency component with a broad peak at the ion plasma

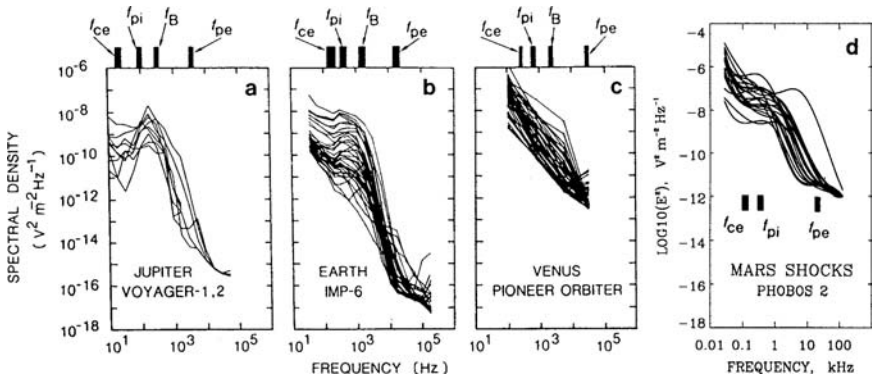


Fig. 3. A comparison between the electric-field spectra measured in the shock ramps of Jupiter, the Earth, Venus and Mars.<sup>13–15</sup>

frequency,  $f_{pi}$ , and then a cutoff, which is thought to be the signature of Doppler-shifted ion acoustic waves.<sup>13</sup>

The electric-field spectra measured in the bow shock ramps of Jupiter, the Earth and Venus are also shown, for comparison, in Fig. 3.<sup>13–15</sup> It is noteworthy that they all show a remarkably close similarity in shape. The noise amplitudes are nevertheless very different. This is partly due to instrumental effects, the antenna lengths are indeed sometimes lower than the plasma Debye length, so that the effective length of such antennae becomes questionable. Moreover, as shown on the third panel from the left, the PVO plasma wave instrument (orbiter electric field detector, OEFD) suffered from a lack of frequency resolution, only four frequency channels (centered on 30 kHz, 5.4 kHz, 730 Hz and 100 Hz) were indeed available.<sup>16</sup> There is therefore a lot to do in this domain, and in particular at Venus.

Electron plasma oscillations have, for the first time, been detected at Mars by PWS. These electrostatic waves are generated, at the plasma frequency, in the electron foreshock by suprathermal electrons that are energized and reflected at the shock whenever the interplanetary magnetic field is connected to the shock surface. Further downstream, in the ion foreshock, ion-acoustic and ULF waves are also generated. Such waves were observed in the Venus electron and ion foreshocks, as shown in Fig. 4.<sup>16</sup> Note that foreshock waves are different to those generated from exospheric ion pick-up.<sup>9</sup>

The spatial distribution of electron plasma oscillations observed at Mars by PWS is displayed in Fig. 5.<sup>17</sup> As expected, the highest electric-field intensities are seen in the electron foreshock. The observed limited extent of plasma oscillations along the tangent magnetic-field line is thought to be the consequence of the small size of the Martian shock. This is consistent with

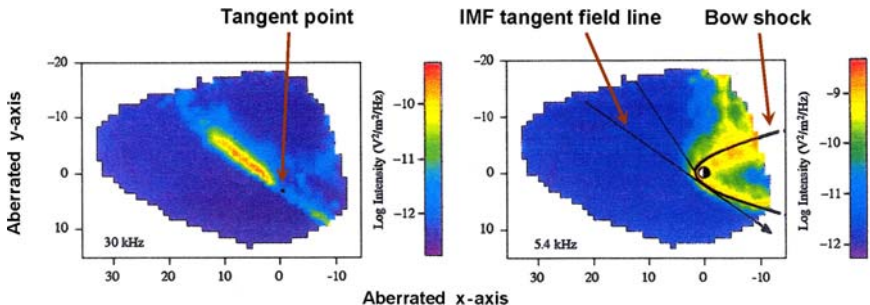


Fig. 4. Electron plasma oscillations (left) and ion acoustic waves (right) in, respectively, the electron and ion foreshocks of Venus.<sup>16</sup>

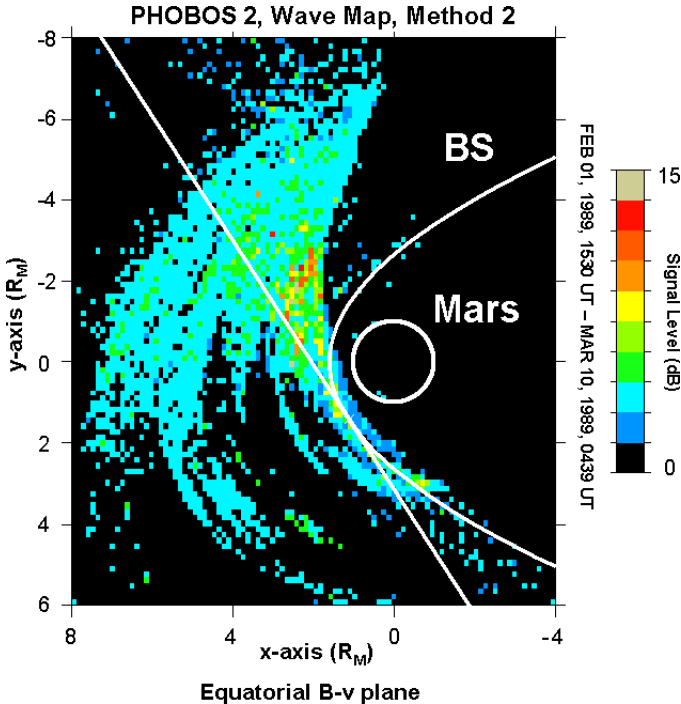


Fig. 5. Electron plasma oscillation intensity in the equatorial  $B-v$  plane, which contains the center of Mars and is parallel both to the solar wind velocity and the interplanetary magnetic field (IMF) line that passes through the spacecraft. The white line, curve and circle are, respectively, the typical Parker IMF line tangent to the shock, the average shock surface, bow shock (BS) and planet Mars.<sup>17</sup>

the argument that the shock curvature controls the electron energization, as is the case for Venus.<sup>16</sup>

### 3.2. Ionosphere and ionopause

The ionospheric plasma composition at Venus is mainly  $O_2^+$  below 200 km and  $O^+$  above. The dayside ionosphere density peak ( $5-7 \times 10^5 \text{ cm}^{-3}$ ) is located at about 140-km altitude, depending on solar activity. It has only been measured by radio-occultation.<sup>18</sup> A precise determination of the ion and electron temperatures remains to be done. The ionosphere upper boundary, the ionopause, is typically located at 300 km in the subsolar direction and at 1000 km close to the terminator, at least, when the solar wind ram pressure does not exceed the ionospheric pressure.<sup>19,20</sup>

Information about the ionosphere of Mars actually comes only from *in situ* measurements made by the two Viking landers (at low latitudes,  $\sim 45^\circ$  SZA, near a minimum of solar activity), and altitude profiles of the electron density obtained from the radio-occultation experiments onboard the Mariner and Viking orbiters.<sup>22</sup> A peak density of  $10^5 \text{ cm}^{-3}$  (about one order of magnitude lower compared with Venus) is usually observed at 125-km altitude. The topside termination of the ionosphere (ionopause) has not been firmly observed. This could be attributed to the fact that, at Mars, the ionospheric thermal plasma pressure is most of the time insufficient to balance the solar wind dynamic pressure.<sup>3</sup> At Venus, when the solar wind dynamic pressure occasionally exceeds the peak ionospheric plasma pressure, no sharp increase of the ionosphere density is indeed observed at the ionopause.<sup>19</sup> The Martian ionosphere is mainly composed of  $\text{O}_2^+$  ions, mostly created by charge exchanges between  $\text{CO}_2^+$  and  $\text{O}_2$ , and between  $\text{CO}_2^+$  and  $\text{O}$ .<sup>23</sup>

Returning now to the fact that, at Mars, the ionospheric thermal plasma pressure is usually lower than the solar wind ram pressure. Luhmann<sup>24</sup> claimed that by analogy with Venus, one might expect to find induced magnetic fields on the surface of Mars that could be detected by ground magnetometers. These fields of external origin should thus combine with crustal *remanent* magnetic fields. At solar maximum, when the solar wind pressure gets very high, large-scale horizontal magnetic fields have been observed in the dayside ionosphere of Venus. They are interplanetary fields incompletely cancelled by the shielding currents in the upper ionosphere. At Mars, these fields could also make their way through the solid mantle of the planet, might be pulled into the wake, and could produce the slingshot magnetic field pattern on the nightside that will accelerate plasma down the tail. It may therefore be the greatest loss source for the Mars atmosphere (C. T. Russell, private communication).

### 3.3. Plasma clouds

Thermal electrons (plasma clouds), possibly scavenged from the top of the ionosphere by Kelvin–Helmholtz instability, were detected in the Venus’ magnetosheath, above the ionopause.<sup>25,26</sup> They could be attached streamers analogous to cometary tails and might be the seed population of suprathermal ions (10–90 eV) that are observed in these regions.

Cold plasma clouds have been observed in the sunward “planetosphere” of Mars (Fig. 6). Densities as high as  $700 \text{ cm}^{-3}$ , and temperatures of the

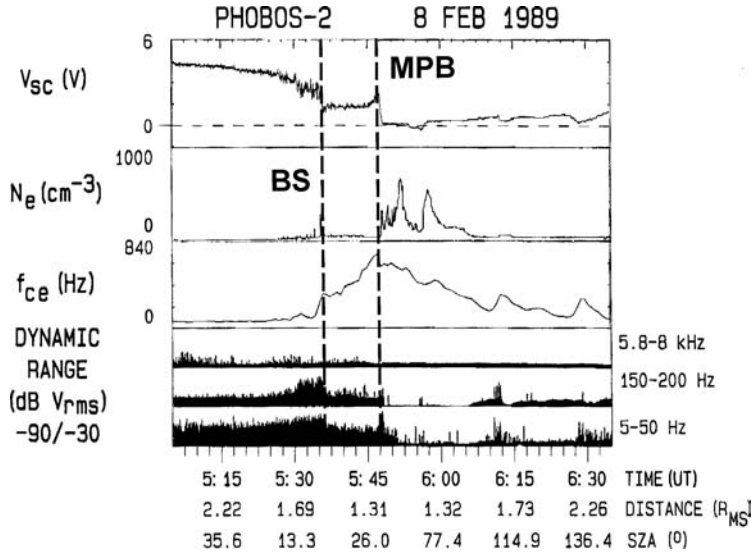


Fig. 6. From top to bottom, spacecraft potential, plasma density, electron gyro-frequency and electric field in three frequency channels measured by the PWS of the Phobos 2 mission to Mars.<sup>15</sup> The bow shock (BS) and magnetic pile-up boundary (MPB) are, respectively, crossed at 0535:50 UT and 0548 UT on 8 February 1989.<sup>21</sup> Plasma clouds are seen just after the MPB.

order of  $10^4$  K have been reported.<sup>15</sup> It is worth noting that the dynamic pressure developed by such clouds is equivalent to that of a 20-nT magnetic field. Plasma clouds could be generated by ionization of plasmaspheric neutrals or could result from ionopause instabilities. They actually look like Venus' cold plasma clouds.

Plasma clouds ( $>60 \text{ cm}^{-3}$ ;  $\sim 1 \text{ eV}$ ) were also observed in the night sector of Mars, close to the neutral sheet, in association with a broadband wave activity (from a few Hz to several kHz). The density profiles of these cold plasma clouds displayed fluctuations correlated with those of the magnetic field. They may originate from the dayside ionosphere and be dragged into the night sector by the solar wind flow. Again, they look like the Venus' plasma clouds and/or tail rays.<sup>27</sup>

### 3.4. Magnetic pile-up boundary

Attempts to characterize the location and shape of the magnetic pile-up boundary (MPB), a boundary in the lower magnetosheath of Mars

(previously called Protonopause, Planetopause, Ion Composition Boundary, Magnetopause, etc.) were first carried out using Phobos 2 data.<sup>21</sup> Then, MGS observations combined with those of Phobos 2 have shown that it is actually a plasma boundary formed by the interaction of the solar wind with the Martian exosphere/ionosphere.<sup>8,11,28</sup>

At Venus, plasmas of solar and planetary origin appear to be separated from each other by a transition region, called mantle (or magnetic barrier), where plasma clouds were seen.<sup>1,26</sup> Recently, Bertucci *et al.*<sup>29</sup> claimed that the upper boundary of this region would be similar to the MPB identified at comets<sup>30,31</sup> and planet Mars.<sup>21,28</sup> The MPB should therefore be a common plasma boundary in the interaction between the solar wind and non-magnetic objects.

#### 4. Conclusion

The solar wind interactions with Venus and Mars appear to be quite similar, but with significant differences.<sup>12,19,32</sup> These differences include a greater width of the Martian bow shock associated with a greater width of magnetotail and a much larger  $O^+$  ion escape rate. The latter is related to a lower Martian gravitational field compared with those of Venus and the Earth, a larger extent of the exosphere, and efficient energizing processes. A relative insensitivity of the Martian bow shock to the solar cycle compared with the unquestionable Venus' bow shock variability has also been reported (Refs. 9 and 32, and references therein).

Any intrinsic B-fields are too weak at Mars and Venus to stand off the solar wind, therefore the atmosphere (exosphere included) and ionosphere combine to provide an obstacle to the flow. Outermost signatures of Mars' and Venus' obstacles are fast magnetosonic shocks and foreshocks. Magnetic pile-up regions of the two planets are dominated by oxygen ions from planetary origin and are bounded outward by the MPB, an internal plasma boundary which could be a common feature of non-magnetized bodies.

Topside termination of the ionosphere (ionopause) is not observed at Mars, it could be because the incident solar wind pressure usually exceeds the ionospheric one. Further analyses (in particular, Mars Express and Venus Express data) and, definitely, *in situ* observations (ESA Cosmic Vision program, other international programs) might yield additional information and most probably contrasts, in particular on the nightside which is, for example, almost unknown at Mars. We indeed do not know if

plasma holes similar to the ones observed at Venus<sup>33,34</sup> are actually present at Mars.

## References

1. C. T. Russell and O. Vaisberg, in *Venus*, eds. D. M. Hunten, L. Colin, T. M. Donahue and V. I. Moroz (University of Arizona Press, Tucson, AZ, USA, 1983), p. 873.
2. J. G. Luhmann, *Space Sci. Rev.* **44** (1986) 241.
3. J. G. Luhmann and L. H. Brace, *Rev. Geophys.* **29** (1991) 121.
4. M. H. Acuña, J. E. P. Connerney, P. Wasilewski, R. P. Lin, K. A. Anderson, C. W. Carlson, J. McFadden, D. W. Curtis, D. Mitchell, H. Rème, C. Mazelle, J. A. Sauvaud, C. d'Huston, A. Cros, J. L. Medale, S. J. Bauer, P. Cloutier, M. Mayhew, D. Winterhalter and N. F. Ness, *Science* **279** (1998) 1676.
5. D. H. Crider, *Adv. Space Res.* **33** (2004) 152.
6. T. K. Breus, S. J. Bauer, A. M. Krymskii and V. Y. Mitniskii, *J. Geophys. Res.* **94** (1989) 2375.
7. J. G. Trotignon, M. Parrot, J. C. Cerisier, M. Menvielle, W. I. Axford, M. Paëtold, R. Warnant and A. W. Wernik, *Planet. Space Sci.* **48** (2000) 1181.
8. A. F. Nagy, D. Winterhalter, K. Sauer, T. E. Cravens, S. Brecht, C. Mazelle, D. Crider, E. Kallio, A. Zakharov, E. Dubinin, M. Verigin, G. Kotova, W. I. Axford, C. Bertucci and J. G. Trotignon, *Space Sci. Rev.* **111** (2004) 33.
9. C. Mazelle, D. Winterhalter, K. Sauer, J. G. Trotignon, M. H. Acuña, K. Baumgärtel, C. Bertucci, D. A. Brain, S. H. Brecht, M. Delva, E. Dubinin, M. Øieroset and J. Slavin, *Space Sci. Rev.* **111** (2004) 115.
10. M. Tatraliyay, C. T. Russell, J. D. Mihalov and A. Barnes, *J. Geophys. Res.* **88** (1983) 5613.
11. J. G. Trotignon, C. Mazelle, C. Bertucci and M. H. Acuña, *Planet. Space Sci.* **54** (2006) 357.
12. J. G. Luhmann, *Adv. Space Res.* **12** (1992) 191.
13. J. G. Trotignon, R. Grard and S. Savin, *J. Geophys. Res.* **96** (1991) 11,253.
14. F. L. Scarf, D. A. Gurnett and W. S. Kurth, *Nature* **292** (1981) 747.
15. R. Grard, C. Nairn, A. Pedersen, S. Klimov, S. Savin, A. Skalsky and J. G. Trotignon, *Planet. Space Sci.* **39** (1991) 89.
16. R. J. Strangeway and G. K. Crawford, *Adv. Space Res.* **16** (1995) 125.
17. J. G. Trotignon, A. Trotignon, E. Dubinin, A. Skalsky, R. Grard and K. Schwingenschuh, *Adv. Space Res.* **26** (2000) 1619.
18. A. J. Kliore, R. Woo, J. W. Armstrong and I. R. Patel, *Science* **203** (1979) 765.
19. J. G. Luhmann, C. T. Russell, F. L. Scarf, L. H. Brace and W. C. Knudsen, *J. Geophys. Res.* **92** (1987) 8545.
20. J. L. Phillips, J. G. Luhmann and C. T. Russell, *J. Geophys. Res.* **89** (1984) 10676.
21. J. G. Trotignon, E. Dubinin, R. Grard, S. Barabash and R. Lundin, *J. Geophys. Res.* **101** (1996) 24,965.

22. M. H. G. Zhang, J. G. Luhmann, A. J. Kliore and J. Kim, *J. Geophys. Res.* **95** (1990) 14,829.
23. W. B. Hanson, S. Sanatani and D. R. Zuccaro, *J. Geophys. Res.* **82** (1977) 4351.
24. J. G. Luhmann, *J. Geophys. Res.* **96** (1991) 18,831.
25. L. H. Brace, R. F. Theis and W. R. Hoegy, *Planet. Space Sci.* **30** (1982) 29.
26. L. H. Brace, H. A. Taylor, Jr., T. I. Gombosi, A. J. Kliore, W. C. Knudsen and A. F. Nagy, in *Venus*, eds. D. M. Hunten, L. Colin, T. M. Donahue and V. I. Moroz (University of Arizona Press, Tucson, AZ, USA, 1983), p. 779.
27. C. M. C. Nairn, R. Grard, A. Skalsky and J. G. Trotignon, *J. Geophys. Res.* **96** (1991) 11,227.
28. C. Bertucci, C. Mazelle, D. H. Crider, D. Vignes, M. H. Acuña, D. L. Mitchell, R. P. Lin, J. E. P. Connerney, H. Rème, P. Cloutier, N. F. Ness and D. Winterhalter, *Geophys. Res. Lett.* **30** (2003) 1099.
29. C. Bertucci, C. Mazelle, J. A. Slavin, C. T. Russell and M. H. Acuña, *Geophys. Res. Lett.* **30** (2003) 1876.
30. F. M. Neubauer, *Astron. Astrophys.* **187** (1987) 73.
31. C. Mazelle, H. Rème, J. A. Sauvaud, C. d'Huston, C. W. Carlson, K. A. Anderson, D. W. Curtis, R. P. Lin, A. Korth, D. A. Mendis, F. M. Neubauer, K. H. Glassmeir and J. Raeder, *Geophys. Res. Lett.* **16** (1989) 1035.
32. C. T. Russell, M. Ong, J. G. Luhmann, K. Schwingenschuh, W. Riedler and Ye. Yeroshenko, *Adv. Space Res.* **12** (1992) 163.
33. L. H. Brace, R. F. Theis, H. G. Mayr, S. A. Curtis and J. G. Luhmann, *J. Geophys. Res.* **87** (1982) 199.
34. H. Pérez-de-Tejada, *J. Geophys. Res.* **106** (2001) 211.